



Hydrological impacts of climate change on small ungauged catchments- results from a GCM-RCM-hydrologic model chain

Aynalem T. Tsegaw¹, Marie Pontoppidan², Erle Kristvik¹, Knut Alfredsen¹, Tone M. Muthanna¹

5 ¹ Department of Civil and Environmental Engineering, Norwegian University of Science and
Technology (NTNU), S.P. Andersensvei 5, N-7491, Trondheim, Norway.

² NORCE Norwegian Research Centre, Bjerknes Centre for Climate Research, Bergen, Norway.

Correspondance to: Aynalem T. Tsegaw (aynaalem.t.tasachew@ntnu.no)

10

Abstract. Climate change is one of the greatest threats to the World's environment. In Norway,
the change will strongly affect the pattern, frequency and magnitudes of stream flows. However,
it is highly challenging to quantify to what extent it will affect flow patterns and floods from small
ungauged rural catchments due to unavailability or inadequacy of hydro-meteorological data for
15 the calibration of hydrological models and tailoring methods to a small-scale level. To provide
meaningful climate impact studies at small catchments, it is therefore beneficial to use high spatial
and temporal resolution climate projections as input to a high-resolution hydrological model. Here
we use such a model chain to assess the impacts of climate change on flow patterns and frequency
of floods in small ungauged rural catchments in western Norway using a new high-resolution
20 regional climate projection, with improved performance with regards to the precipitation
distribution, and the regionalized hydrological model (Distance Distribution Dynamics) between
the reference period (1981-2011) and a future period (2071-2100). The FDCs of all study
catchments show there will be more wetter periods in the future than the reference period. The
results also show that in the future period, the mean annual flow increases by 16.5% to 33.3%, and
25 there will be an increase in the mean autumn, mean winter and mean spring flows ranging from



4.3% to 256.3%. The mean summer flow decreases by 7.2% to 35.2%. The mean annual maximum floods increase by 28.9% to 38.3%, and floods of 2 to 200 years return periods increase by 16.1% to 42.7%. The findings of this study could be of practical use to regional decision-makers if considered alongside other previous and future findings.

30

1 Introduction

Climate change is one of the greatest threats to human existence, economic activity, ecosystems and civil infrastructures (Kim and Choi, 2012). Climate change risks for natural and human systems are higher for global warming of 1.5 °C than at present, but lower than at 2 °C, and these risks depend on the magnitude and rate of warming, geographic location, levels of development, vulnerability, and on the choices and implementation of adaptation and mitigation options (IPCC, 2018). The trend of changes in different parts of Europe may vary considerably because of changes in large-scale atmospheric circulation or local orographic circulation (Eisenreich et al., 2005, Hattermann et al., 2007)..

40

Changes in temperature and precipitation and the shift in winter precipitation from snow to rain will be crucial in studying impacts of climate change on hydrology of a catchment. These changes influence the hydrological regime of a stream, and the most serious and widespread potential impact of the changes is flooding (Baltas, 2007, Richardson, 2002, Thornes, 2001). In Norway, the average annual temperature and precipitation are expected to increase by 3.8 °C to 6.2 °C and 7% to 27% respectively by the end of the century using RCP8.5 emission scenario (Hanssen-Bauer et al., 2015). The largest increases in precipitation are mostly expected during the autumn and winter



months and will in turn impact the magnitude and in some cases the seasonality of peak runoff and floods. A climate impact study at Sogn and Fjordane county of Norway showed that flood peaks
50 shifted from summer to autumn for the future scenario (Chernet et al., 2014), and Donnelly et al. (2017) studied climate change impacts on European hydrology and found that in the Norwegian region, climate change will strongly affect the hydrological cycle in the future period. Also, outside Norway, authors have reported that the frequency and magnitude of flows are being affected by the changes in climatic conditions (Alfieri et al., 2015; Madsen et al., 2014; Mallakpour &
55 Villarini, 2015; Rojas et al., 2013). Climate change adverse results upon streamflow regimes worldwide (Pumo et al., 2016), calls for attention of the impact study on a local scale.

Projected increase in the frequency and intensity of heavy localized precipitation events, based on climate models, contributes to increasing in precipitation-generated local flooding, and an increase
60 in local sudden flooding is causing significant danger and loss of life and property (Borga et al., 2011, Kundzewicz et al., 2014). Local sudden floods (flash floods) usually occur in small catchments (e.g., catchments less than 100 – 1000 km²). This type of flood event is usually short in duration, but it is usually connected with severe damage (Menzel et al., 2006). Studies show that the probability and magnitude of hazardous heavy precipitation events have been increasing
65 in several European regions e.g., (Golz et al., 2016). Heavy localized precipitation could be caused by low pressure system (e.g., western Norway (Azad and Sorteberg, 2017)) or because of prevailing convective precipitation at hilly or mountainous areas.

A quantitative analysis of the impacts of climate change on flooding conditions requires
70 simulations of climatological-hydrological system. The models on which the simulations are based



should give an adequate representation of the system dynamics relevant for different types of flow (e.g. floods) generation (Menzel et al., 2006). The climate and hydrological models are the two models involved in climatological-hydrological system. Climate change affects the basic components of hydrologic cycles, and the application of hydrological models provide the means
75 to conceptualize and investigate the relationship between climate (e.g. precipitation and temperature) and water resources (e.g. low flows and floods) of a region to assess the likely effects of climate change and propose appropriate adaptation strategies (Baltas, 2007). The regional impacts of climate change (e.g. on local flooding) come out with the necessity of orienting adaptation measures to local climatic, geographic, economic and social conditions (Hattermann,
80 2009, Krysanova et al., 2008). Because catchment storage (e.g. effective lake, soil and groundwater) has a significant role in altering the timing between the precipitation and runoff, the relationship between projected changes in precipitation and corresponding runoff cannot be compared directly. Therefore, hydrological modelling based on a local climate scenario is required to assess the impact that changes in precipitation and temperature will have on processes leading
85 to different types of flows (e.g. floods) (Lawrence et al., 2012). This is generally performed by following a sequence of steps from global and regional climate modelling, through data tailoring (downscaling and bias-adjustment) and hydrological modelling (Olsson et al., 2016).

Climate impact assessment on hydrology of small ungauged catchments using continuous
90 hydrological modelling is challenging because of unavailability or inadequacy of hydro-meteorological data for calibration of hydrological models, short response time of the catchments, difficulty in describing local hydrological processes and coarse resolution of climate models. The challenge in coarse spatial resolution of climate models is due to poor representation of



precipitation which is inadequate for assessment of impacts on smaller catchments (Quintero et
95 al., 2018). For example, Pontoppidan et al. (2017) showed that during a flooding event in western
Norway, the regional model simulated observed rainfall considerably better with a grid spacing of
3 km compared to a grid spacing of 9 km due to the complex terrain in the area. Therefore,
to provide a meaningful climate impact results at small catchments, it is necessary to use high
spatial and temporal resolutions of projected climate data that can be used as forcing in
100 high resolution hydrological models (Lespinas et al., 2014; López-Moreno et al., 2013; Reynolds
et al., 2015; Tofiq & Guven, 2014). Current efforts of coordinated regional downscaling in Europe
(EURO-CORDEX e.g. (Jacob et al., 2014; Kotlarski et al., 2014)) are performed on a 0.11° grid,
however a new high-resolution regional downscaling with improved representation of local
precipitation distribution for southern Norway is available (Pontoppidan et al., 2018), but has yet
105 to be included in a full hydrological model chain.

To solve the challenge related to lack of availability of a properly calibrated high-resolution
hydrological model at ungauged small rural catchments in Norway, a predictive tool has been
developed and tested. Tsegaw et al. (2019a) calibrated and validated Distance Distribution
110 Dynamics (DDD) hydrological model at forty-one gauged small rural catchments in Norway with
hourly temporal resolution. For predicting flow at ungauged catchments, the DDD model
parameters have been regionalized using three methods of regionalization (multiple regression,
physical similarity and combined method) and the methods have been tested on seven independent
catchments. The finding shows that the combined method performs the best of all the methods in
115 predicating flow. Even if the DDD model predicts flow at ungauged catchments satisfactory (0.5
 \leq Kling-Gupta Efficiency < 0.75), the model underestimates most of the observed flood peaks. To



improve the prediction of observed floods, a dynamic river network method has been introduced and implemented in DDD (Tsegaw et al., 2019b). This improved setup has been used in this study where the general objective is to assess the hydrological impacts of climate change on small ungauged catchments using a novel model chain consisting of a high resolution, bias corrected dynamical downscaling and the improved DDD model. We specifically focus on:

- i. Assessing the impacts of climate change on the changes of flow patterns at ungauged small rural catchments around Bergen, Norway.
- ii. Assessing impacts of climate change on the pattern and frequency of floods in ungauged small rural catchments around Bergen, Norway.

The knowledge gained is critical for decision makers so that flood risk management strategies can be planned accordingly and in a timing manner.

2 Data and methods

2.1 Study area

Six ungauged small rural catchments, located in western Norway around Bergen, are used in this study. We selected the catchments using <http://nevina.nve.no/> and <https://www.norgeskart.no/>. The definition of small rural catchments is based on the report of Fleig and Wilson (2013) with an upper area limit of 50km². The catchments are selected for the impact study because there are critical infrastructures (e.g. culverts, bridges and buildings) at the outlet of the catchments which could be affected by the climate change in the future period. We selected three catchments with bare mountain dominated (>50%) and three catchments with forest dominated (>50%) to include diverse land uses in the study. The locations and observed river networks of the selected



catchments are depicted in Fig. 1. The catchment descriptors (CDs) and outlet coordinates of each
140 study catchment are presented in Table 1.

2.2 Climate, topography and land use data

The precipitation and temperature data used to drive the hydrological model are obtained from a
simulation performed by the Weather Research and Forecasting model (WRF) version 3.8.1
145 (Skamarock et al., 2008). The model is non-hydrostatic and widely used for weather forecasting
and research purposes. The simulation has a spatial grid resolution of 4 km x 4 km and the
precipitation and temperature are available every 3 hours. However, regional models, as WRF,
inherit biases from the boundary conditions used to drive the model. These biases may lead to
misrepresentation of important features in the models, e.g. the known bias of the North Atlantic
150 storm track (Zappa et al., 2013) leads individual storms into central Europe instead of a more
northern path along the Norwegian coast as observations suggest. Therefore, the global climate
model NorESM1-M used as forcing data at the boundaries in WRF was corrected for such biases
before the regional downscaling. This led to a more realistic representation of the North Atlantic
storm track and the precipitation distribution in southern Norway (Pontoppidan et al., 2018).

155

The DDD model parameters, which do not need calibration, are derived from an analysis of hydro-
meteorological, topographical and land use data of a catchment using GIS. The source of the
topography and land use data is the Norwegian Mapping Authority (www.statkart.no). The 10m x
10 m DEM, the river network and the 1: 50 000 scale land use data have been retrieved and used
160 in the study. The DEM has been re-conditioned to the naturally occurring river network using the
Arc-hydro tool to create a hydrologically correct terrain model that can improve the accuracy of



watershed modeling (Li, 2014). The re-conditioned DEM is further used to determine the distance distributions of hill slopes and river networks as needed by DDD.

165 2.3 DDD hydrological model

The Distance Distribution Dynamics (DDD) hydrological model is developed by Skaugen and Onof (2014) and currently runs operationally with daily and three-hourly time steps at the Norwegian flood forecasting service. It has two main modules: the subsurface and the dynamics of runoff.

170 2.3.1 The Subsurface

The volume capacity of the subsurface water reservoir, M (mm), is shared between a saturated zone with volume, S (mm), and an unsaturated zone with volume, D (mm). The volume of the saturated zone and the unsaturated zone are inversely related i.e. the higher the unsaturated zone volume, the lower the saturated zone (Skaugen and Mengistu, 2016, Skaugen and Onof, 2014).

175 The actual water volume present in the unsaturated zone is described as Z (mm). The subsurface state variables are updated after evaluating whether the current soil moisture, $Z(t)$, together with the input snowmelt and rain, $G(t)$, represent an excess of water over the field capacity, R , which is fixed at 30 % of $D(t)$ i.e. $R = 0.3$ (Skaugen and Onof, 2014). If $G(t) + Z(t) > R \cdot D(t)$, then the excess water $X(t)$ is added to $S(t)$.

180 Excess water
$$X(t) = \text{Max} \left\{ \frac{G(t)+Z(t)}{D(t)} - R, 0 \right\} D(t) \quad \left[\frac{\text{mm}}{3\text{hours}} \right] \quad (1)$$

Groundwater
$$\frac{dS}{dt} = X(t) - Q(t) \quad \left[\frac{\text{mm}}{3\text{hours}} \right] \quad (2)$$

Soil water content
$$\frac{dZ}{dt} = G(t) - X(t) - Ea(t) \quad \left[\frac{\text{mm}}{3\text{hours}} \right] \quad (3)$$



Soil water zone $\frac{dD}{dt} = -\frac{dS}{dt}$ $\left[\frac{mm}{3hours} \right]$ (4)

Potential evapotranspiration $Ep = Cea * T$ $\left[\frac{mm}{3hours} \right]$ (5)

185 Actual evapotranspiration $Ea = Ep * \frac{S+Z}{M}$ $\left[\frac{mm}{3hours} \right]$ (6)

2.3.2 Runoff dynamics

The dynamics of runoff in DDD has been derived from the catchment topography using a GIS combined with runoff recession analysis. In DDD, the distribution of distances between points in the catchment and their nearest river reach (distance distributions of a hillslope) is the basis for describing the flow dynamics of the hillslope. The distribution of distances between points in the river network and the outlet forms the basis for describing the flow dynamics of the river network. The hillslope and river flow dynamics of DDD is hence described by unit hydrographs (UHs) derived from distance distributions from a GIS and celerity derived from recession analysis (Skaugen and Mengistu, 2016, Skaugen and Onof, 2014). When the distance distributions are associated with flow celerity of the hillslope and rivers, we obtain the distributions of travel times which constitutes the time area concentration curve (Maidment, 1993). The derivative of the time area concentration curve gives an instantaneous unit hydrograph (UH) (Bras, 1990), which is basically a set of weights distributing the input (precipitation and snowmelt) in time to the outlet.

200

Previous studies in more than 120 catchments in Norway showed that the exponential distribution describes the hillslope distance (Euclidean distance from the nearest river reach) distribution well, and the normal distribution describes well the distances between points in the river network and outlet of a catchment (Skaugen and Onof, 2014). Figure 2 shows the structure of the DDD model.



205 The model is written in the R programming language. All GIS work is done with ArcGIS 10.3
(ESRI, 2014), and the recession analysis is done using a R script (R Core Team, 2017) .

2.3.3 Dynamic river network method in DDD

Dynamic expansions and contractions of stream networks play an important role for hydrologic
210 processes since they connect different parts of the catchment to the outlet (Nhim, 2012). Dynamic
river networks and hence dynamic overland unit hydrographs are introduced and implemented in
the DDD model to improve the simulation of floods (Tsegaw et al., 2019b). The mean of the
distribution of distances from a point in the catchment to the nearest river reach (D_m) becomes
dynamic in the dynamic river network method. We therefore need to estimate the dynamic D_m
215 from the relation between upstream critical supporting area (A_c) i.e. the area needed to initiate and
maintain streams and D_m using GIS as shown in Eq.(7). Coefficients a and b are estimated for each
study catchments and are presented in Table 2. The calibration parameter of the dynamic river
network routine in DDD is critical flux (F_c) and is estimated by regional regression.

$$D_m = aA_c^b \quad (7)$$



220 **2.3.4 Model parameters**

The DDD model parameters are divided into three main groups. The first group are those estimated from observed hydro-meteorological data (for gauged catchments) or through regionalization for ungauged catchments (appendix 1), the second group are those estimated by model calibration (for gauged catchments) against observed discharge or by regionalization methods (for ungauged
225 catchments) (appendix 2), and the third group are those estimated from digitized geographic maps using a GIS (appendix 3). The snow routine in DDD has two parameters estimated from the spatial distribution of observed precipitation data (Skaugen and Weltzien, 2016). The shape parameter (a_0) and the decorrelation length (d) of the gamma distribution of snow and snow water equivalent (SWE) are estimated from a previous calibration for 84 catchments in Norway (Skaugen et al.,
230 2015). Since our study focuses on ungauged catchments, we cannot conduct calibration, and we therefore derived the model parameters needing calibration through combined method of regionalization using 41 gauged small rural catchments in Norway as a base (Tsegaw et al., 2019a).

2.3.5 Regionalizing the parameters of DDD model

235 To estimate the regionalized parameters for this study (3 hourly time step), we have used the combined method of regionalization which has been recommended for estimating regionalized DDD model parameters with hourly resolution (Tsegaw et al., 2019a). In the combined method of regionalization, we have estimated the recession parameters and critical flux using multiple regression between model parameters and CDs, and the other parameters (all in appendix 2) using
240 the physical similarity method with pooled donor catchments. The parameters of the model needing regionalization are shown in appendix 1 and 2 (the bottom 5 parameters in appendix 1 and all in appendix 2).



245 The CDs of the study catchments, used for multiple regression, are presented in Table 1. The multiple regression equations used in this study are taken from the above-mentioned references and presented below.

$$Gscale = \exp(-5.12 - 0.12Le + 0.22 \ln(S_q) + 0.3 \log(M_e)) \quad (8)$$

$$Gshape = 0.82 + 0.0005M_p - 0.009S_q \quad (9)$$

250 $Gshl = 2.047Gshape - 0.658 \quad (10)$

$$GscI = 0.49Gscale - 0.0014 \quad (11)$$

$$f_c = 160.7 - 1.4B \quad (12)$$

The parameters of DDD model needing calibration are estimated using a pooling-group type of physical similarity method of regionalization. Kay et al. (2006) defined physical similarity using
255 Euclidean distance in a space of CDs as shown in Eq.13.

$$dist_{a,b} = \sqrt{\sum_{j=1}^J \left(\frac{X_{a,j} - X_{b,j}}{\sigma_{x,j}} \right)^2} \quad (13)$$

Where j indicates one of a total of 12 CDs (all in Table 1 except outlet locations), $X_{a,j}$ is the value of that CD at the a^{th} ungauged catchment (the six catchments in Table 1), $X_{b,j}$ is the value of the
260 CD at b^{th} catchment which is a member of the 41 calibrated catchments studied in Tsegaw et al.



(2019a) , and $\sigma_{x,j}$ is the standard deviation of the CD across all the 41 catchments. Seven closest neighbor catchments (minimum distance) are selected to create a pooling group. After identifying the pooling group members, we have computed the model parameter at the ungauged catchment a (α_a^{PG}) as a weighted average of the parameters of the 7 members. Kay et al. (2007) stated that it is more appropriate to write the expression for the model parameter as a weighted average of the estimated parameter values, α_m , for all 41 catchments (N) as shown in Eq. (14).

$$\alpha_a^{PG} = \frac{\sum_{m=1}^N h_{am} \alpha_m}{\sum_{m=1}^N h_{am}} \quad (14)$$

Catchments not in the pooling group are given a weight h_{am} equal to zero, but those in the pooling are assigned weights to reflect their importance which is based on the distance measure $dist_{a,b}$ as defined in Eq. (13). The weights of the pooling group members are estimated by Eq. (15).

$$h_{am} = 1 - S_{am} \quad (15)$$

where

$$S_{am} = \frac{dist_{a,b}}{dist_{a,max}} \quad (16)$$

where $dist_{a,max}$ is set to be 10% larger than the maximum distance of a pooling group member from the ungauged catchment a .

2.4 Impact study

We have extracted the precipitation and temperature data from the 4 X 4 km and 3 hourly resolution climate model. The climate data are forced into the DDD model to simulate the runoff,



280 actual evapotranspiration and snow water equivalent (SWE) both for the reference and future
periods. We have used 30 hydrological years (1st of September to 31st of August) for both periods
of the impact study. We have analyzed changes of the following climate impact indicators:

- i) The mean annual changes of precipitation, temperature, flow, snow water equivalent (SWE) and actual evapotranspiration.
- 285 ii) The mean annual and mean seasonal changes of flow
- iii) The annual and seasonal flow duration curves (FDCs)
- iv) The timing of annual winter/spring and fall stream flow
- v) The mean annual and seasonal maximum flows
- vi) Floods with return periods of 2 to 200 years

290 Changes are computed by Eq. (17) using the magnitudes of hydro-climatic variable for the
reference and future periods.

$$\text{Change in } x(\%) = \left(\frac{\text{Future value of } x - \text{Reference value of } x}{\text{Reference value of } x} \right) * 100 \quad (17)$$

where x is any hydro-climatic variable.

295 **2.4.1 Changes of hydro-climatic elements**

The 3 hourly precipitation and temperature data, extracted from the climate model, are analyzed
using an R-script to quantify the changes in the mean annual values for the reference and future
periods. The 3-hourly precipitation data are aggregated yearly to estimate the annual precipitation
value and then averaged over the 30 years to get the mean annual value. The 3-hourly temperature
300 data are averaged for the whole 30 years to estimate the mean annual temperature. The simulated



3-hourly flow is averaged for the whole 30 years to get the mean annual flow data. Seasonal mean flow data are also estimated for the reference and future periods i.e. winter, spring, summer and autumn for assessing changes in the seasonal mean flow. The annual maximum SWE is selected from each hydrological year and averaged for reference and future periods to get the mean annual maximum SWE for the two periods. The annual actual evapotranspiration is estimated by aggregating the actual evapotranspiration from the 3-hour simulation results and then averaged over 30 years to get the mean annual actual evapotranspiration.

2.4.2 Changes in flow duration curves

A flow duration curve is a cumulative curve that shows the percent of time a specified flow is equaled or exceeded during a given period, and it shows the flow characteristic of a stream throughout a range of flow, without regard to the sequence of occurrence (Searcy, 1959). We have analyzed changes in the stream flow variability over a water year between the reference and future periods. The changes of floods (between 0% and 10% exceedance), medium flows (between 10% and 70% exceedance) and low flows (between 70% and 100% exceedance) are analyzed in this study. The formula to calculate the probability of exceedance is given by Eq. (18).

$$p = 100 * \frac{K}{(n + 1)} \quad (18)$$

p = the probability that a given flow will be equaled or exceeded (% of time)

K = the ranked position on the listing (dimensionless)

n = the number of events for period of record, and it is dimensionless



2.4.3 Changes in timing of annual winter/spring and fall stream flow

The annual timing of river flows is a good indicator of climate-related changes. Changes in timing of annual winter/spring (WS) and fall stream flow is analyzed using center of volume date
325 (Hodgkins et al., 2003). The center of volume date is the date by which half of the total volume of water for a given period flows by a river section. The center of volume date is expected to be more robust indicator of the timing of the bulk of high flows in a season than the peak flows, as the peak flow may happen before or after the bulk of seasonal flows (Hodgkins et al., 2003). From the 3-hour flow data (simulated for the reference and future periods), we have calculated the mean 3-
330 hour flow for the 30 years in both periods. Using the mean 3-hour flow, we have computed seasonal center of volume dates for the winter/spring (1 January to 31 May) and fall (1 October to 31 December).

2.4.4 Changes in the maximum flows and flood frequency

335 The annual and seasonal maximum flows (floods) are selected from the 30 years of reference and future periods for the analysis. The changes in the mean and median of the annual and seasonal maximum flows are analyzed.

The number of 3-hour floods (frequency) above a certain threshold helps us to have a general overview on the impacts of climate change on the flood risk in small catchments. Accordingly, we
340 have analyzed the changes in the number of 3-hour floods between the reference and future periods with a flow higher than the minimum of the 30 years annual maximum flow for the reference period.



To assess the magnitude of a flood with a given probability, flood frequency methods must be
345 applied. Flood frequency analysis is important for flood hazard mapping, for which a flood of a
certain return period (e.g. 200 years in Norway) is used for the flood zone mapping (Groen et al.,
2012). To analyse changes in the magnitudes of a flood with a given return period (e.g. 200-year
flood), flood frequency analysis is applied to the annual maximum series for the reference (1981
– 2011) and future periods (1970 – 2100). The percentage change in the flood magnitude is then
350 computed as the difference between the two curves divided by the flood magnitude for the
reference period. We have used a Gumbel distribution (Bhagat, 2017, Shaw, 1983) to model the
annual maximum series in this study. We have selected the Gumbel distribution because it has
been widely applied including the studies of climate change impacts on floods in Europe (Dankers
and Feyen, 2008, Veijalainen et al., 2010).

355

3 Results

3.1 Regionalized DDD model parameters

The results of the parameters values from the regionalization for the six study catchments are
presented in Table 3. The parameters and possible ranges of values are presented in appendix 4.

360 3.2 Changes in hydro-climatic elements

The simulation results of the hydrological model are further analyzed to quantify the changes in
the hydro-climatic elements. The mean annual precipitation, the mean annual temperature, the
mean annual evapotranspiration, the mean annual flow, the mean autumn flow, and the mean
winter flow increase for all the study catchments in the future period compared to the reference
365 period. The mean spring flow increases in the five catchments and decrease in one study



catchment. The mean summer flow decreases for the five catchments. The mean annual maximum SWE decreases for all the study catchments. In the future period, the mean annual precipitation increases by 20% to 23.9 %. The mean annual temperature rises in 3 - 3.3 degree Celsius. The mean annual flow increases from 16.5% to 33.3%. The decrease in the mean summer flow ranges from 7.2% to 35.2% and the increase is 3.6% in only one of the study catchments. The mean winter flow increases by an average of 126.9% (ranging from 41.3% to 256.3%). The mean spring flow increases by 4.3% to 99.7% for the five catchments and there will be a decrease by 1.4% in one catchment. The mean autumn flow increases by an average of 37% (ranging from 20.6% to 43.9%). The results of changes of the mean annual temperature, precipitation, maximum SWE and actual evapotranspiration are presented in Table 4. Table 5 presents changes in the mean annual and seasonal flows for the catchments. Mean 3 hourly flow of the study catchments are shown in Fig. 3 for the reference and future periods.

3.3 Changes in flow duration curves

The results of the study show that changes in the flow duration curves (FDCs) values are positive for all the flow conditions. The FDC values of the future period increase for all flow conditions (low, medium and high flows) for all the study catchments. For all catchments, the top 5% of flows in the future period are higher than the reference period by 7.6% to 61.5%. The median flow (flows which are exceeded by 50% of the time) increases by 23.7% to 139.6% (the highest value is for catchment 1 and the lowest value is for catchment 4) in the future period. Figure 4 shows the FDCs for both periods.



3.4 Changes in timing of annual winter/spring (WS) and fall stream flow

For all the study catchments, the mean WS center of volume dates occur earlier in the future period
390 (16 - 68 days) than the reference period. The fall CV date occurs later for all the study catchments
in the future period and a shift of 1 – 16 days is expected. Table 6 presents the mean WS CV dates
and mean fall CV dates for all the study catchments.

3.5 Changes in the maximum flows and flood frequency

395 3.5.1 Changes in the annual and seasonal maximum flows

The annual and seasonal maximum flows increase in the future period compared to the reference
period. The mean annual maximum flows increase from 28.9% to 38.3% across all the study
catchments. The mean seasonal maximum flows also show an increase in all seasons (1.1 % to
118%) and all catchments except for spring season of catchment 2 (reduction of 28.9%) as shown
400 in Table 7. The median of the annual and seasonal maximum flows increases for all catchments
except for spring season of catchment 2 as shown in Fig.5. Table 7 presents the results of changes
in the mean annual and seasonal maximum flows in future period compared to the reference period.
Figure 5 shows the distributions of the 30 years annual and seasonal maximum flows both for the
reference and future periods.

405

The number of 3-hours with floods exceeding the minimum annual maximum flood in the 30 years
of the reference period increases in the future period significantly (Table 8). This result shows that



flooding will occur more often in the future period. In the future period, the yearly average number of such floods increase between 61.7% to 133% across all study catchments.

410 **3.5.2 Changes in flood frequencies**

The flood frequency analysis using Gumbel's Extreme Value Distribution shows that floods of 2, 5, 10, 20, 25, 50, 100 and 200 years return periods increase in the future period (2070 – 2100) compared to the reference period (1981 – 2011) for all catchments. The increase ranges from 16.1% to 42.7%. Table 9 shows the changes of flood frequencies for the selected return periods
415 for all the study catchments.

4 Discussion

4.1 Regionalized DDD model parameters

When we estimate the DDD model parameters needing calibration using the pooling group method
420 of regionalization for the ungauged study catchments, many of the most similar gauged catchments (from the 41 database) are found to be in the western Norway (west climate region) and close to the ungauged study catchments which shows that the regionalization method used in this study is plausible.

4.2 Hydrological impacts of climate change

425 **4.2.1 Changes of hydro-climatic elements**

Generally, the findings of the increase in precipitation and temperature for the study catchments are in the range of increments predicted by the Norwegian Center for Climate Services (NCCS) under the report Climate in Norway 2100 (Hanssen-Bauer et al., 2015) ; however the results from



some catchments are above or below the prediction interval of the report since the comparison is
430 between catchments specific results with the regional values of the report. The NCCS report is
based upon ten climate models with RCP8.5 and RCP4.5 using daily temporal resolution, and we
have compared our findings with the RCP8.5 results of the report. The report shows that there will
be an increase of precipitation by 2.5% to 21% for the Hordaland county of Norway (where our
study catchments are located) between 1971-2000 and 2071 – 2100 and there will be an increase
435 of temperature by 3.1 to 4.9 degree Celsius for ensembles of RCP 8.5. The results of the climate
model in our study are generally in agreement with the aforementioned report i.e. changes of 20%
- 23.9% and 3-3.3 degree Celsius for precipitation and temperature respectively; however, the
results from the climate model used in this study predicts precipitation changes to the higher end
of the climate service report and the temperature changes towards the lower end of the climate
440 service report. In the future period, all the study catchments show an increase in the mean annual
flow when compared to the reference period. The maximum increase is 33.3%, and the minimum
increase is 16.5%. Alcamo et al. (2007) found that mean annual river flow projected to increase in
northern Europe (e.g. Norway) by approximately 9% to 22% up to the 2070 which aligns with our
findings i.e. the increment could increase by 16.5% up to 33.3 % to 2100. The increase in mean
445 annual flow (mean annual water volume) in the future period is a result of a substantial increase in
projection of the mean annual precipitation with a moderate increase in mean temperature i.e. the
mean annual precipitation increases by 20% to 23.9% while the mean annual temperature increases
by 3°C to 3.3°C (Table 4). The increase in the mean annual temperature results in an increase of
water loss by evapotranspiration. However, the mean annual increase in precipitation exceeds the
450 mean annual increase in the actual evapotranspiration (43% to 131.5%) and these conditions
contributed to increase of mean annual flow in general. The Climate in Norway 2100 report shows



that the mean annual flow for western Norway (where the study catchments are located) could increase from -1% to 17% in 2100 and our result shows that the increase is slightly higher than the increase in the report for four of the study catchments. This could be related to the capability of the climate model used in this study to reflect the local representation of precipitation and temperature, the differences in the temporal resolution used by this study and the report and the averaging issue in estimating the regional value by the report.

Unlike the changes in the mean annual flow, changes in the temporal distribution of flows (e.g. seasonal) can be important because changes are rarely identical throughout the year (Olsson et al., 2016). The mean winter and autumn flows increase for all study catchments. The main causes of increases are projected increase in the precipitation and temperature during the autumn and winter seasons. The increase in mean winter flow contributes to much of the increase in the mean annual flow for all catchments (Table 5 and Fig.3). The main cause of increase in the mean winter flow is increased winter temperatures. Increased winter temperatures result in a higher proportion of winter precipitation to fall as rain which then results in a higher proportion of winter flow. The mean spring flows show an increase for the five catchments and a decrease for one catchment while the mean summer flows show a decrease for the five catchments and an increase for one of the catchments.

470

Similar results are found in other hydrological assessments of the Bergen region. Previous studies of the water resources in Bergen under climate change also project higher temperatures and increased annual precipitation in the Bergen region for the 2071-2100 future period under the



RCP8.5 emissions scenario (Kristvik et al., 2018, Kristvik and Riisnes, 2015). Kristvik et al. (2018)
475 based their assessment on statistical downscaling of an ensemble of RCPs and GCMs, followed
by simulations of the hydrological response in term of inflow to surface water reservoirs. Due to
higher temperatures and more rainfall precipitation, strong increases in winter flow was found,
while a decrease was projected in spring/summer months due to less snowmelt (Kristvik et al.
2018).

480

The climate in Norway 2100 report for western Norway shows that the mean winter and autumn
flow increase by 15% to 42% and by 5% to 36% respectively in 2100. The findings of this study
show that the increase in mean winter flow is higher than the maximum prediction in the report
for four catchments and to the higher end of the prediction in the report for the remaining two
485 catchments. Similar results have been obtained for mean autumn flows except that three
catchments have higher value than the maximum prediction value in the report. The report predicts
an increase of the mean spring flow by -9% to 17% and a decrease of mean summer flow by 13%
to 28% in 2100. The findings of this study show that the increase in the mean spring flow is within
the prediction interval of the report for three catchments and higher than the maximum prediction
490 value of the report for the rest three catchments. The results of this study show a higher decrease
than the maximum prediction in the report for the three catchments and lower decrease than the
minimum prediction in the report for two catchments. Only one catchment shows a decrease with
in the prediction interval of the report. Wong et al. (2011) studied the differences in hydrological
drought characteristics in summer season of Norway between the periods 1961-1990 and 2071-
495 2100 using HBV hydrological model with daily temporal resolution and found that substantial
increases in hydrological drought duration and drought affected areas are expected in Norway



which aligns with our findings. Ministry of the Environment of Norway (2009) also pointed out that the summer flow in Norway is projected to be reduced and supports the findings of our study.

500 Climate change affects snow pack and the amount of water stored in the snow pack (SWE). Increased winter temperature will generally lead to a reduction in snow storage and hence the mean maximum SWE will also reduce in the future. The results of this study show that there will be a reduction in the mean maximum SWE at all the catchments in the future period. The reduction ranges from 47.5% to 77.8%. The largest reduction is found to be at the catchment with the highest
505 mean elevation value (catchment 1). Snow accumulation and its characteristics are the results of air temperature, precipitation, wind and the amount of moisture in the atmosphere. Therefore, changes in these and other climatic properties can affect snow pack and hence maximum SWE. In our study, there is an increase in precipitation and temperatures for all study catchments in the future period, and the increase resulted in the reduction of mean annual maximum SWE at all the
510 study catchments.

4.2.2 Changes in Flow duration curves (FDCs)

The results of this study show that climate change affects the FDCs of the study catchments. The future FDC is higher than the FDC of the reference period at all catchments for all probability of
515 exceedances (Fig.4). The FDCs of all the study catchment show that the low flows increase in the future, and there will be more wetter periods in the future than in the reference period.



4.2.3 Changes in WSCV and fall CV dates

The mean winter/spring center of volume date (WSCV) will be earlier, and the mean fall CV date
520 will be later for all the study catchments. The change in WSCV dates is related to the amount and
timing of spring snowmelt and warmer winter temperature. The earlier mean WSCV date in the
future period is the result of increased precipitation falling during a warmer winter, reduced snow
storage, early snow melt and warmer spring temperature. The late occurrence of fall CV dates is
related to the higher precipitation and temperature projected in fall in the future period. The warmer
525 temperature in the future period makes the major proportion of future precipitation to fall as rain
which in turn increases the total flow volume in fall which makes the fall CV dates to occur later.

4.3 Changes in the maximum flows and flood frequency

4.3.1 Annual and seasonal maximum flows

530 In the future period (2070 – 2100), the results of this study show that there will be an increase in
the mean and median of the annual and seasonal maximum flows (Table 7 and 8 and Fig.5) at all
the study catchments except for the spring season of catchment 2. Many (15 – 23 of the 30 annual
maximum floods) of the maximum annual flows happen during the autumn period (1st September
to 30th of November) and therefore much of the contribution for the increment of the mean and
535 median annual maximum flows comes from the autumn (Fig.5). The second higher contribution
for the increment of the mean and median annual maximum flows is winter season (Fig.5). In the
future period, the winter maximum flows increase in magnitude and frequencies as a substantial
amount of precipitation falls as rain in a warmer climate. The mean summer maximum flows show
the least increment in the future period (1.1% to 20.7%), but the summer season contributes to the



540 increment of the mean and median of the annual maximum flows (the third higher contributor to
the annual maximum flows). The mean spring maximum flows show the highest increment in
percentage (25.4% to 118% for five of the study catchments and 28.9% reduction for one of the
study catchments) compared to the other seasons, but the contribution of the spring season for the
mean and median increment of the annual maximum flows is the least of all the seasons. The
545 finding that mean annual maximum flows (floods) increase by 28.9% to 38.3% in our study is
supported by Lawrence and Hisdal (2011). Lawrence and Hisdal (2011) have done ensemble
modelling based on locally adjusted precipitation and temperature data from 13 regional climate
scenarios to assess likely changes in hydrological floods between a reference period (1960 – 1990)
and two future periods (2021-2050) and (2071 - 2100), for the 115 catchments distributed
550 throughout in Norway. Their results showed that western regions of Norway are associated with
the largest percentage increases in the magnitude of the mean annual floods (> 20%). Lawrence
and Hisdal (2011) also pointed out that increase in autumn and winter rainfall throughout Norway
will increase the magnitude of peak flows during these seasons, and at areas already dominated by
autumn and winter floods, the projected increases in floods magnitude will be large. Since our
555 study catchments are at western Norway which is dominated by autumn floods and our finding
(Fig.5) confirms their finding in that the maximum increases in floods magnitude are expected to
happen in autumn and winter seasons (Table 7 and Fig.5).

The yearly average number of 3-hours flows, which are greater than the minimum of the annual
560 maximum high flows in the 30 years of the reference period increases. The yearly average number
of such floods increase between 61.7% and 133% across all study catchments as presented in Table
8. The results show that there will be a greater number of 3-hours floods in the future period than



the reference period, and more flood risks are expected at the infrastructures constructed downstream of small ungauged rural catchments in west coast Norway near Bergen city. European
565 Environmental Agency(2004b), in: Alcamo et al. (2007) found that the risk of floods increases in northern Europe (e.g. Norway) which supports our finding of increase in the risk of floods. Center for International Climate Research (<https://cicero.oslo.no>) predicts that western Norway will experience more heavy rain and flooding in the future and our findings confirms their predictions.

570 **4.3.2 Changes in flood frequency analysis**

The study results from the six ungauged small catchments show that there will be an increase in flood frequencies with a return periods of 2, 5, 10, 20, 25, 50, 100, 200 years in the future period. The changes of all return periods for all catchments are in between 16.1% and 42.7%. The maximum and the minimum changes happen for a return period of 200 years. For all return periods,
575 the mean changes are between 31 % and 32% while the median changes are between 30% and 34%. The 2, 5, 10 years changes are greater than 20% for all catchments and 20, 25, 50, 100 and 200-years changes are greater than 20% for five of the six study catchments.

Beldring et al. (2006) studied the percentage change in the mean annual flood and the 50-year
580 flood in four catchments in Norway between 1961-1990 and 2070-2100 in which one of the catchments is in western Norway (Viksvatn in Gaular) and found that moderate to large increases are expected. Their result is supported by our finding i.e. the 50-year flood on six small catchments in west Norway will increase by 18.2% to 40 % between 1981 -2011 and 2070-2100. In our study results, the 200-year flood changes are 16.1%, 34.7%, 41.3%, 42.7%, 31.1% and 22.7% for



585 catchments 1, 2, 3, 4, 5, 6 respectively. Lawrence and Hisdal (2011) have found that the projected
increase of the 200-year flood exceed 40% for some of the catchments in western Norway between
the 1961-1990 reference period and the 2071- 2100 future period which is in agreement with our
findings. Lawrence (2016) used ensembles of regional climate projections from EURO-CORDEX
together with HBV model to assess possible effects of climate change on floods on 115 catchments
590 in Norway for two future periods (20131-2016 and 2071-2100). The assessment result shows that
the minimum increase in the 200 years flood for catchments less than 100km² at Hordaland county
(where the study catchments are located) is 20% which is generally in agreement with our findings.

4.4 Limitations

595 A possible uncertainty related to hydrological modelling in this study is that we have used the
regionalization model developed for 1 hour (Tsegaw et al., 2019a) to estimate parameters for the
3-hour simulation used in this study. DDD model parameters like degree hour factor for
evapotranspiration (Cea) and degree hour factors for snow melt (Cx) can be sensitive to the
temporal resolution. As presented in Table 4, the mean annual actual evaporation value has smaller
600 result than what is expected for Norway which is the result of low value of Cea. However, the
same uncertainty is present both in the reference and future periods. A second possible limitation
is that DDD model parameters are assumed to be constant under changing climatic conditions, and
the same parameter sets are used for the reference and future period simulations. However, studies
show that using the same parameter sets for the reference and future periods under climate impact
605 studies can have significant impact on the simulation results. Merz et al. (2011) found that the
impact on simulated flow of assuming time invariant hydrological model parameters can be very
significant. Thirdly, the modelled changes in the hydro-climatic elements and flood frequency are



derived from a single GCM-RCM model chain, however this simulation has the benefit of a high spatial resolution for a better representation of small-scale features and additionally a novel bias
610 correction method has been applied. Other combinations of GCMs and RCMs predict varieties of future climate change signals which could potentially result in different hydro-climatic and flood predictions for the same study catchments. Ensemble simulations are needed to fully understand and address the uncertainties of future changes in the hydroclimatic elements, however a single model study, like we have used in this study, increases our knowledge and understanding.
615 Therefore, the results of this study alone should not be taken as a conclusive of what will be seen in the future but could be of practical use to regional decision-makers if considered alongside other previous and future findings.

5 Conclusion

620 In this study we use a bias corrected dynamical downscaling product as input for the DDD model to investigate the impact of climate change on small ungauged catchments. The results show that there will be an increase in the mean annual flow in the future period. The increase in the mean annual flow is due to the increase in the mean autumn, winter and spring flows in the future period (2070-2100) compared to the reference period (1981 - 2011). In the future period, the mean
625 summer flows from the study catchments decrease. Future flow duration curves are higher than the flow duration curves of the reference period for all study catchments for all probability of exceedances. The median flow (flows which are exceeded by 50% of the time) increases by 23.7% to 139.6%. The FDCs of all the study catchment show that the low flows increase in the future, and there will be more wetter periods in the future than in the reference period.



630

There will be an increase in the mean annual floods and flood frequencies of 2, 5, 10, 20, 25, 50, 100 and 200 years in the future period. The mean annual maximum floods increase by 28.9% to 38.3%. This study gives clear indication that the projected increase in flood frequencies are high (e.g. 200-year flood > 40%) in small catchments around Berge area of western Norway, and such catchments are vulnerable to an increased risk in the future climate. The high-resolution regional climate model with a novel bias correction method improves the knowledge and understanding of climate change impacts on hydrology of small catchments in western Norway. However, it is important to conduct further researches which can address the limitations of this study before conducting flood risk assessment and planning flood risk management strategies as a national strategy for climate change adaptation.

640

These simulations are based on high resolution regional climate model projection with a novel bias correction method and address limitations in previous impact studies where such projections have not yet been available and enabling in-depth analysis of the impacts of climate change on rapid hydrological processes. An ensemble of GCM-RCM runs building on the results of this paper is suggested as a venue for further work in order to account for uncertainties in future emissions and climate projections and thus provide more reliable recommendations for infrastructure design and adaptation.

645

650



Acknowledgments

The authors would like to acknowledge Norwegian Climate Service Centre for providing information on how to access and process the 3 X 3 km spatial and 3-hours temporal resolution
655 gridded precipitation and temperature climate data for western Norway. The authors also would like to acknowledge Thomas Skaugen of the Norwegian Water Resources and Energy Directorate (NVE) for providing the source code of Distance Distribution Dynamics hydrological model. Finally, the authors gratefully acknowledge the financial support by Bingo and ExtndBingo project (EU Horizon 2020, grant agreement 641739), and the Research Council of Norway (RCN) through
660 R3 (grant 255397) and through the Centre for Research-based Innovation “Klima 2050” (see www.klima2050.no).



References

- 665 Alcamo, J., FlÖRke, M., and MÄRker, M.: Future long-term changes in global water resources driven by socio-economic and climatic changes, *Hydrological Sciences Journal*, 52, 247-275, <https://doi.org/210.1623/hysj.1652.1622.1247>, 2007.
- 670 Alfieri, L., Burek, P., Feyen, L., and Forzieri, G.: Global warming increases the frequency of river floods in Europe, *Hydrol. Earth Syst. Sci.*, 19, 2247-2260, <https://doi.org/2210.5194/hess-2219-2247-2015>, 2015.
- 675 Azad, R. and Sorteberg, A.: Extreme daily precipitation in coastal western Norway and the link to atmospheric rivers, *Journal of Geophysical Research: Atmospheres*, 122, 2080-2095, <https://doi.org/2010.1002/2016JD025615>, 2017.
- 680 Baltas, E. A.: Impact of Climate Change on the Hydrological Regime and Water Resources in the Basin of Siatista, *International Journal of Water Resources Development*, 23, 501-518, <https://doi.org/510.1080/07900620701485980>, 2007.
- 685 Beldring, S., Roald, L. A., Engen-Skaugen, T., and FÖrland, E. J.: Climate Change Impacts on Hydrological Processes in Norway 2071-2100. Based on RegClim HIRHAM and Rossby Centre RCAO Regional Climate Model Results. Norwegian Water Resources and Energy Directorate, Oslo, Norway, 2006.
- 690 Bhagat, N.: Flood Frequency Analysis Using Gumbel's Distribution Method: A Case Study of Lower Mahi Basin, India, *Ocean Development and International Law*, 6, 51-54, <https://doi.org/10.11648/j.wros.20170604.20170611>, 2017.
- 695 Borga, M., Anagnostou, E. N., Blöschl, G., and Creutin, J. D.: Flash flood forecasting, warning and risk management: the HYDRATE project, *Environmental Science and Policy*, 14, 834-844, <https://doi.org/810.1016/j.envsci.2011.1005.1017>, 2011.
- 700 Bras, R. L.: *Hydrology: An Introduction to Hydrologic Science*, Addison-Wesley, 1990.
- 705 Chernet, H. H., Alfredsen, K., and Midttømme, G. H.: Safety of Hydropower Dams in a Changing Climate, *Journal of Hydrologic Engineering*, 19, 569-582, [https://doi.org/510.1061/\(ASCE\)HE.1943-5584.0000836](https://doi.org/510.1061/(ASCE)HE.1943-5584.0000836), 2014.
- 710 Dankers, R. and Feyen, L.: Climate Change Impact on Flood Hazard in Europe: An Assessment Based on High-Resolution Climate Simulations, *Journal of Geophysical Research*, 113, D19105, <https://doi.org/19110.11029/12007JD009719>, 2008.
- 715 Donnelly, C., Greuell, W., Andersson, J., Gerten, D., Pisacane, G., Roudier, P., and Ludwig, F.: Impacts of climate change on European hydrology at 1.5, 2 and 3 degrees mean global warming above preindustrial level, *Climatic Change*, 143, 13-26, <http://dx.doi.org/10.1007/s10584-10017-12022-10580>, 2017.



- 710 Eisenreich, S., Bernasconi, C., and Campostrini, P.: Climate change and the European water dimension, 2005.
- ESRI: ArcGISDesktop Help 10.3 Geostatistical Analyst, doi: <https://www.esri.com/en-us/home>, 2014. 2014.
- 715 Fleig, A. K. and Wilson, D.: Flood estimation in small catchments : literature study. In: Naturfareprosjektet,, Rapport (Norges vassdrags- og energidirektorat : online), Norwegian Water Resources and Energy Directorate, Oslo, 2013.
- 720 Golz, S., Naumann, T., Neubert, M., and Günther, B.: Heavy rainfall: An underestimated environmental risk for buildings?, E3S Web of Conferences, 7, 08001, <https://doi.org/08010.01051/e08003sconf/20160708001>, 2016.
- 725 Groen, R., M. Jespersen, K. de Jong, and Olsson, J.: Climate change impacts and uncertainties in flood risk management: Examples from the North Sea Region. Norwegian Water Resources and Energy Directorate Oslo, 2012.
- Hanssen-Bauer, I., E.J. Førland, I. Haddeland, H. Hisdal, S. Mayer, A. Nesje, J.E.Ø. Nilsen, S. Sandven, A.B. Sandø, and Ådlandsvik, A. S. o. B.: KLIMA I NORGE 2100. Miljø Direktoratet,Oslo, 2015.
- 730 Hattermann, F., Kundzewicz, Z., Becker, C., Castelletti, A., Gooch, G., Kaden, S., de Lange, W., Laurans, Y., Muhar, S., Pahl-Wostl, C., Soncini-Sessa, R., Stålnacke, P., and Willems, P.: Water Framework Directive: Model supported Implementation. A Water Manager's Guide, 2009.
- 735 Hodgkins, G. A., Dudley, R., and Huntington, T.: Changes in the Timing of High River Flows in New England Over the 20th Century, 2003.
- 740 IPCC: Summary for Policymakers. In: Global Warming of 1.5°C. An IPCC Special Report on the impacts of global warming of 1.5°C above pre-industrial levels and related global greenhouse gas emission pathways, in the context of strengthening the global response to the threat of climate change, sustainable development, and efforts to eradicate poverty [Masson-Delmotte, V., P. Zhai, H.-O. Pörtner, D. Roberts, J. Skea, P.R. Shukla, A. Pirani, W. Moufouma-Okia, C. Péan, R. Pidcock, S. Connors, J.B.R. Matthews, Y. Chen, X. Zhou, M.I. Gomis, E. Lonnoy, T. Maycock, M. Tignor, and T. Waterfield (eds.)] World Meteorological Organization, Geneva, Switzerland, 32 pp., **2018**.
- 745 Jacob, D., Petersen, J., Eggert, B., Alias, A., Christensen, O. B., Bouwer, L. M., Braun, A., Colette, A., Déqué, M., Georgievski, G., Georgopoulou, E., Gobiet, A., Menut, L., Nikulin, G., Haensler, A., Hempelmann, N., Jones, C., Keuler, K., Kovats, S., Kröner, N., Kotlarski, S., Kriegsmann, A., Martin, E., van Meijgaard, E., Moseley, C., Pfeifer, S., Preuschmann, S., Radermacher, C., Radtke, K., Rechid, D., Rounsevell, M., Samuelsson, P., Somot, S., Soussana, J.-F., Teichmann, C., 750 Valentini, R., Vautard, R., Weber, B., and Yiou, P.: EURO-CORDEX: new high-resolution climate change projections for European impact research, Regional Environmental Change, 14, 563-578, <http://dx.doi.org/510.1007/s10113-10014-10587-y>, 2014.



755 Kay, A. L., Jones, D. A., Crooks, S. M., Calver, A., and Reynard, N. S.: A comparison of three approaches to spatial generalization of rainfall–runoff models, *Hydrological Processes*, 20, 3953–3973, <https://doi.org/3910.1002/hyp.6550>, 2006.

760 Kay, A. L., Jones, D. A., Crooks, S. M., Kjeldsen, T. R., and Fung, C. F.: An investigation of site-similarity approaches to generalisation of a rainfall–runoff model, *Hydrol. Earth Syst. Sci.*, 11, 500–515, <https://doi.org/510.5194/hess-5111-5500-2007>, 2007.

765 Kim, E. S. and Choi, H. I.: Estimation of the relative severity of floods in small ungauged catchments for preliminary observations on flash flood preparedness: a case study in Korea, *Int J Environ Res Public Health*, 9, 1507–1522, <https://doi.org/1510.3390/ijerph9041507>, 2012.

770 Kotlarski, S., Keuler, K., Christensen, O. B., Colette, A., Déqué, M., Gobiet, A., Goergen, K., Jacob, D., Lüthi, D., van Meijgaard, E., Nikulin, G., Schär, C., Teichmann, C., Vautard, R., Warrach-Sagi, K., and Wulfmeyer, V.: Regional climate modeling on European scales: a joint standard evaluation of the EURO-CORDEX RCM ensemble, *Geosci. Model Dev.*, 7, 1297–1333, <https://doi.org/1210.5194/gmd-1297-1297-2014>, 2014.

775 Kristvik, E., Muthanna, T. M., and Alfreksen, K.: Assessment of future water availability under climate change, considering scenarios for population growth and ageing infrastructure, *Journal of Water and Climate Change*, 10, 1–12, <https://doi.org/10.2166/wcc.2018.2096>, 2018.

Kristvik, E., & Riisnes, B., *Hydrological Assessment of Water Resources in Bergen*. Masters thesis, Norwegian University of Science and Technology, Trondheim, Norway, 2015

780 Krysanova, V., Vetter, T., and Hattermann, F.: Detection of change in drought frequency in the Elbe basin: comparison of three methods, *Hydrological Sciences Journal*, 53, 519–537, <https://doi.org/510.1623/hysj.1653.1623.1519>, 2008.

785 Kundzewicz, Z. W., Kanae, S., Seneviratne, S. I., Handmer, J., Nicholls, N., Peduzzi, P., Mechler, R., Bouwer, L. M., Arnell, N., Mach, K., Muir-Wood, R., Brakenridge, G. R., Kron, W., Benito, G., Honda, Y., Takahashi, K., and Sherstyukov, B.: Flood risk and climate change: global and regional perspectives, *Hydrological Sciences Journal*, 59, 1–28, <https://doi.org/10.1080/02626667.02622013.02857411>, 2014.

790 Lawrence, D.: Klimaendring og framtidige flommer i Norge. avdeling, H. (Ed.), *Norges vassdrags- og energidirektorat*, Oslo, 2016.

Lawrence, D. and Hisdal, H.: *Hydrological projections for floods in Norway under a future climate*, Norwegian Water Resources and Energy Directorate, Oslo, 2011.

795 Lespinas, F., Ludwig, W., and Heussner, S.: Hydrological and climatic uncertainties associated with modeling the impact of climate change on water resources of small Mediterranean coastal rivers, *Journal of Hydrology*, 511, 403–422, <https://doi.org/410.1016/j.jhydrol.2014.1001.1033>, 2014.



- 800 Li, Z.: Watershed modeling using arc hydro based on DEMs: a case study in Jackpine watershed, *Environmental Systems Research*, 3, 1-11, <https://doi.org/10.1186/2193-2697-1183-1111>, 2014.
- López-Moreno, J. I., Pomeroy, J. W., Revuelto, J., and Vicente-Serrano, S. M.: Response of snow processes to climate change: spatial variability in a small basin in the Spanish Pyrenees, *Hydrological Processes*, 27, 2637-2650, <https://doi.org/2610.1002/hyp.9408>, 2013.
- 805 Madsen, H., Lawrence, D., Lang, M., Martinkova, M., and Kjeldsen, T. R.: Review of trend analysis and climate change projections of extreme precipitation and floods in Europe, *Journal of Hydrology*, 519, 3634-3650, <https://doi.org/3610.1016/j.jhydrol.2014.3611.3003>, 2014.
- 810 Maidment, D. R.: Developing a spatially distributed unit hydrograph by using GIS, *IAHS Publication 211*: 181 - 192, 1993.
- Mallakpour, I. and Villarini, G.: The changing nature of flooding across the central United States, *Nature Climate Change*, 5, 250-254, <https://doi.org/210.1038/nclimate2516>, 2015.
- 815 Menzel, L., Niehoff, D., Bürger, G., and Bronstert, A.: Climate change impacts on river flooding: A modelling study of three meso-scale catchments, *Climatic Change: Implications for the Hydrological Cycle and for Water Management*, 10, 249-269, https://doi.org/210.1007/1000-1306-47983-47984_47914 2006.
- 820 Merz, R., Parajka, J., and Blöschl, G.: Time stability of catchment model parameters: Implications for climate impact analyses, *Water Resources Research - WATER RESOUR RES*, 47, W02531, <https://doi.org/02510.01029/02010WR009505>, 2011.
- 825 Ministry of the Environment of Norway: Norway's Fifth National Report under the United Nation's Framework Convention on Climate Change. 2009.
- Nhim, T.: Variability of intermittent headwater streams in boreal landscape : Influence of different discharge conditions, Student thesis, Examensarbete vid Institutionen för geovetenskaper, 39 pp., 2012.
- 830 Olsson, J., Arheimer, B., Borris, M., Donnelly, C., Foster, K., Nikulin, G., Persson, M., Perttu, A.-M., Uvo, C. B., Viklander, M., and Yang, W.: Hydrological Climate Change Impact Assessment at Small and Large Scales: Key Messages from Recent Progress in Sweden, *Climate*, 4, 39, <https://doi.org/10.3390/cli4030039>, 2016.
- 835 Pontoppidan, M., Kolstad, E. W., Sobolowski, S., and King, M. P.: Improving the Reliability and Added Value of Dynamical Downscaling via Correction of Large-Scale Errors: A Norwegian Perspective, *Journal of Geophysical Research: Atmospheres*, 123, 11,875-811, 888, <https://doi.org/810.1029/2018JD028372>, 2018.
- 840



- 845 Pontoppidan, M., Reuder, J., Mayer, S., and Kolstad, E. W.: Downscaling an intense precipitation event in complex terrain: the importance of high grid resolution, *Tellus A: Dynamic Meteorology and Oceanography*, 69, 1271561, <https://doi.org/10.1016/j.tellsta.2017.11.001>, 2017.
- 850 Pumo, D., Caracciolo, D., Viola, F., and Noto, L. V.: Climate change effects on the hydrological regime of small non-perennial river basins, *Science of The Total Environment*, 542, 76-92, <https://doi.org/10.1016/j.scitotenv.2015.10.1109>, 2016.
- 855 Quintero, F., Mantilla, R., Anderson, C., Claman, D., and Krajewski, W.: Assessment of Changes in Flood Frequency Due to the Effects of Climate Change: Implications for Engineering Design, *Hydrology*, 5, 1-19, <https://doi.org/10.3390/hydrology5010019>, 2018.
- R Core Team: R: A Language and Environment for Statistical Computing, doi: <http://www.R-project.org/>, 2017. 2017.
- 860 Richardson, D.: Flood risk—the impact of climate change, *Proceedings of the Institution of Civil Engineers - Civil Engineering*, 150, 22-24, <https://doi.org/10.1680/cien.2002.1150.1685.1622>, 2002.
- 865 Rojas, R., Feyen, L., and Watkiss, P.: Climate change and river floods in the European Union: Socio-economic consequences and the costs and benefits of adaptation, *Global Environmental Change*, 23, 1737-1751, <https://doi.org/10.1016/j.gloenvcha.2013.1708.1006>, 2013.
- Searcy, J.: Flow-Duration Curves, 1959.
- 870 Skamarock, W. C., Klemp, J., Dudhia, J., Gill, D. O., Barker, D., and Wang, W.: A Description of the Advanced Research WRF Version 3, University Corporation for Atmospheric Research. , 27, 3-27, <https://doi.org/10.5065/D5068S5064MVH>, 2008.
- 875 Skaugen, T. and Mengistu, Z.: Estimating catchment-scale groundwater dynamics from recession analysis – enhanced constraining of hydrological models, *Hydrol. Earth Syst. Sci.*, 20, 4963-4981, <https://doi.org/10.5194/hess-4920-4963-2016>, 2016.
- 880 Skaugen, T. and Onof, C.: A rainfall-runoff model parameterized from GIS and runoff data, *Hydrological Processes*, 28, 4529-4542, <https://doi.org/10.1002/hyp.9968>, 2014.
- Skaugen, T., Peerebom, I. O., and Nilsson, A.: Use of a parsimonious rainfall–run-off model for predicting hydrological response in ungauged basins, *Hydrological Processes*, 29, 1999-2013, <https://doi.org/10.1002/hyp.10315>, 2015.
- 885 Skaugen, T. and Weltzien, I. H.: A model for the spatial distribution of snow water equivalent parameterized from the spatial variability of precipitation, *The Cryosphere*, 10, 1947-1963, <https://doi.org/10.5194/tc-1910-1947-2016>, 2016.



890 Thornes, J. E.: IPCC, 2001: Climate change 2001: impacts, adaptation and vulnerability,
Contribution of Working Group II to the Third Assessment Report of the Intergovernmental Panel
on Climate Change, edited by J. J. McCarthy, O. F. Canziani, N. A. Leary, D. J. Dokken and K. S.
White (eds). Cambridge University Press, Cambridge, UK, and New York, USA, 2001, ISBN 0-
521-01500-6 (paperback), ISBN 0-521-80768-9 (hardback), International Journal of Climatology,
895 22, 1285-1286, <https://doi.org/1210.1002/joc.1775>, 2002.

Tofiq, F. A. and Guven, A.: Prediction of design flood discharge by statistical downscaling and
General Circulation Models, Journal of Hydrology, 517, 1145-1153,
<https://doi.org/1110.1016/j.jhydrol.2014.1106.1028> 2014.

900 Tsegaw, A. T., Alfredsen, K., Skaugen, T., and Muthanna, T. M.: Predicting hourly flows at
ungauged small rural catchments using a parsimonious hydrological model, Journal of Hydrology,
573, 855-871, <https://doi.org/810.1016/j.jhydrol.2019.1003.1090>, 2019a.

905 Tsegaw, A. T., Skaugen, T., Alfredsen, K., and Muthanna, T. M.: A dynamic river network method
for the prediction of floods using a parsimonious rainfall-runoff model, Hydrology Research,
2019b. <https://doi.org/10.2166/nh.2019.2003>, 2019b.

910 Veijalainen, N., Lotsari, E., Alho, P., Vehviläinen, B., and Käyhkö, J.: National Scale Assessment
of Climate Change Impacts on Flooding in Finland, Journal of Hydrology, 391, 333-350,
<https://doi.org/310.1016/j.jhydrol.2010.1007.1035>, 2010.

915 Wong, W. K., Beldring, S., Engen-Skaugen, T., Haddeland, I., and Hisdal, H.: Climate Change
Effects on Spatiotemporal Patterns of Hydroclimatological Summer Droughts in Norway, Journal
of Hydrometeorology, 12, 1205-1220, <https://www.jstor.org/stable/24912722>, 2011.

Zappa, G., Shaffrey, L., and Hodges, K.: The Ability of CMIP5 Models to Simulate North Atlantic
Extratropical Cyclones*, Journal of Climate, 26, 5379-5396, <https://doi.org/5310.1175/JCLI-D-5312-00501.00501>, 2013.

920

925



Appendixes

Appendix 1. List of DDD model parameters estimated from observed precipitation data and those estimated from regionalization (multiple regression) for the study catchments.

Parameters	Description of the parameter	Method of estimation	Unit
d	Parameter for spatial distribution of SWE, decorrelation length	From spatial distribution of observed precipitation	Positive real number
a0	Parameter for spatial distribution of SWE, shape parameter	From spatial distribution of observed precipitation	Positive real number
MAD	Long term mean annual discharge	Specific runoff map of Norway	m ³ sec ⁻¹
Gshape	Shape parameter of λ	Regression	Positive real number
Gscale	Scale parameter of λ	Regression	Positive real number
GshInt	Shape parameter of Λ	Regression	Positive real number
GscInt	Scale parameter of Λ	Regression	Positive real number
Fc	Critical flux	Regression	m ³ /hour

930



Appendix 2. List of DDD rainfall-runoff model parameters estimated from pooling group of
 935 physical similarity method of regionalizations.

Parameters	Description of the parameter	Method of estimation	Unit
Pro	Liquid water in snow	Regionalization (poolig group)	fraction
940 Cx	Degree hour factor for snow melt	Regionalization (poolig group)	mm °C ⁻¹ hour ⁻¹
CFR	Degree hour factor for refreezing	Regionalization (poolig group)	mm °C ⁻¹ hour ⁻¹
Cea	Degree hour factor for evapotranspiration	Regionalization (poolig group)	mm °C ⁻¹ hour ⁻¹
rv	Celerity for river flow	Regionalization (poolig group)	m/s

945

950



Appendix 3. List of DDD rainfall-runoff model parameters estimated from geographical data using GIS.

Symbol of parameters	Description of the Parameter
area	Catchment area
maxLbog	Maximum distance of marsh land portion of hillslope
midLbog	Mean distance of marsh land portion of hillslope
bogfrac	Areal fraction of marsh land from the total land uses
zsoil	Areal fraction of DD for soils (what area with distance zero to the river)
zbog	Areal fraction of distance distribution for marsh land (what area with distance zero to the river)
midFl	Mean distance (from distance distribution) for river network
stdFL	Standard deviation of distance (from distance distribution) for river network
maxFL	Maximum distance (from distance distribution) for river network
maxDI	Maximum distance (from distance distribution) of non-marsh land (soils) of hill slope
midDL	Mean distance (from distance distribution) of non-marsh land (soils) of hill slope
midGl	Mean distance (from distance distribution) for Glacial
stdGl	Standard deviation of distance (from distance distribution) for Glacial
maxGl	Maximum distance (from distance distribution) for Glacial
Hypsographic curve	11 values describing the quantiles 0, 10, 20, 30, 40, 50, 60,70,80,90,100



Appendix 4. Possible ranges of regionalized DDD model parameters

Model parameters needing regionalization	Method of regionalization	Possible ranges of values
Gshape	Multiple regression	Positive real number
Gscale	Multiple regression	Positive real number
GshInt	Multiple regression	Positive real number
GscInt	Multiple regression	Positive real number
fc	Multiple regression	Positive real number
Pro	Pooling group type of physical similarity	0.03 - 0.1
Cx	Pooling group type of physical similarity	0.05 - 1.0
CFR	Pooling group type of physical similarity	0.001 - 0.01
Cea	Pooling group type of physical similarity	0.01 - 0.1
rv	Pooling group type of physical similarity	0.5 - 1.5



Figure Captions

Figure 1. Locations of study catchments in Norway

Figure 2. Structure of the Distance Distributions Dynamics model adapted from Skaugen and Onof (2014). Left panel: the storage model and right panel: hydrographs of hillslope and river

Figure 3. Yearly mean 3 hourly hydrographs of the study catchments for the reference and future periods

Figure 4: Flow duration curves (FDCs) of the 3-hourly flow for the six study catchments both for the reference and future periods

Figure 5. Distributions of the annual and seasonal maximum flow values of the 30 years period



Figures

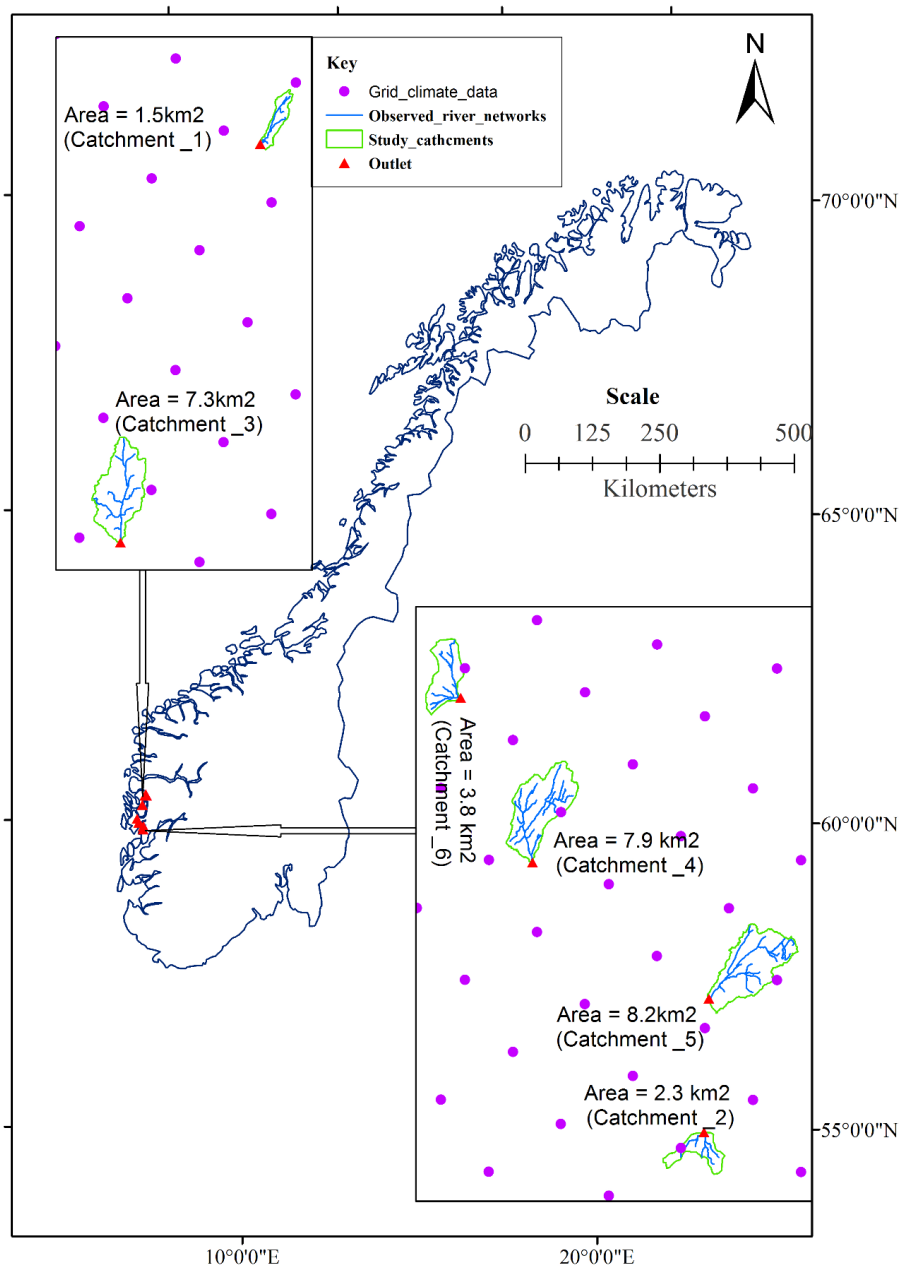


Figure 1. Locations of study catchments in Norway.

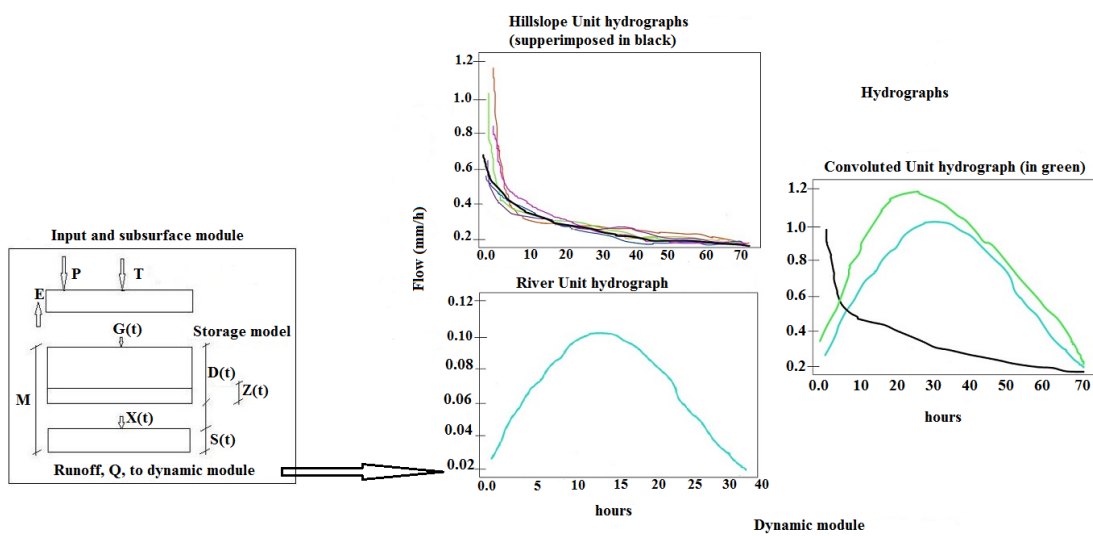


Figure 2. Structure of the Distance Distributions Dynamics model adapted from Skaugen and Onof (2014). Left panel: the storage model and right panel: hydrographs of hillslope and river.

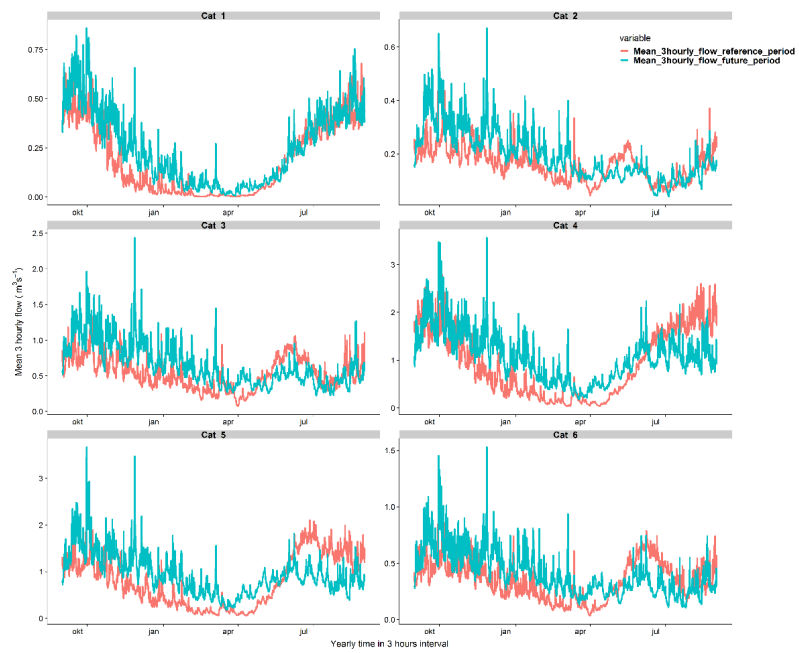


Figure 3. Yearly mean 3 hourly hydrographs of the study catchments for the reference and future periods

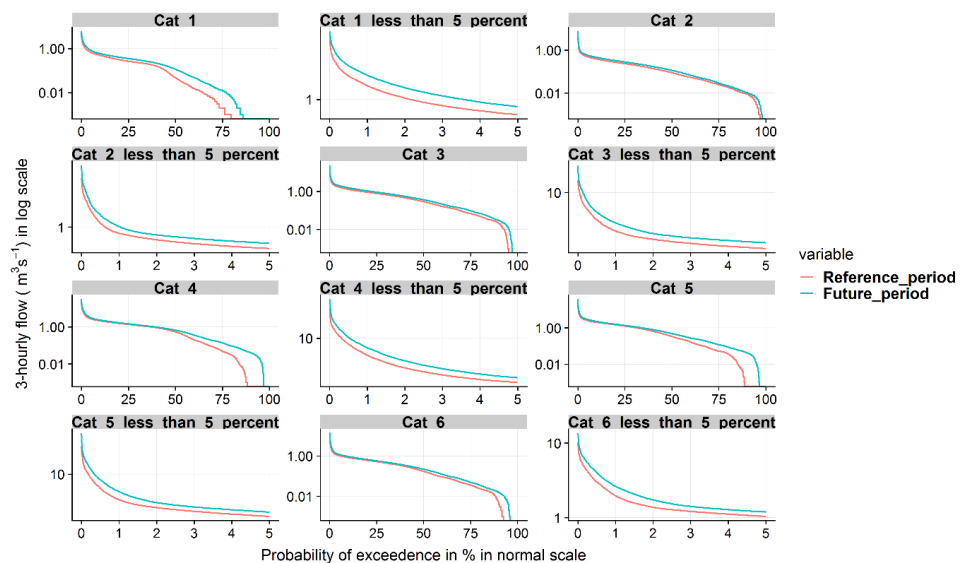


Figure 4: Flow duration curves (FDCs) of the 3-hourly flow for the six study catchments both for the reference and future periods

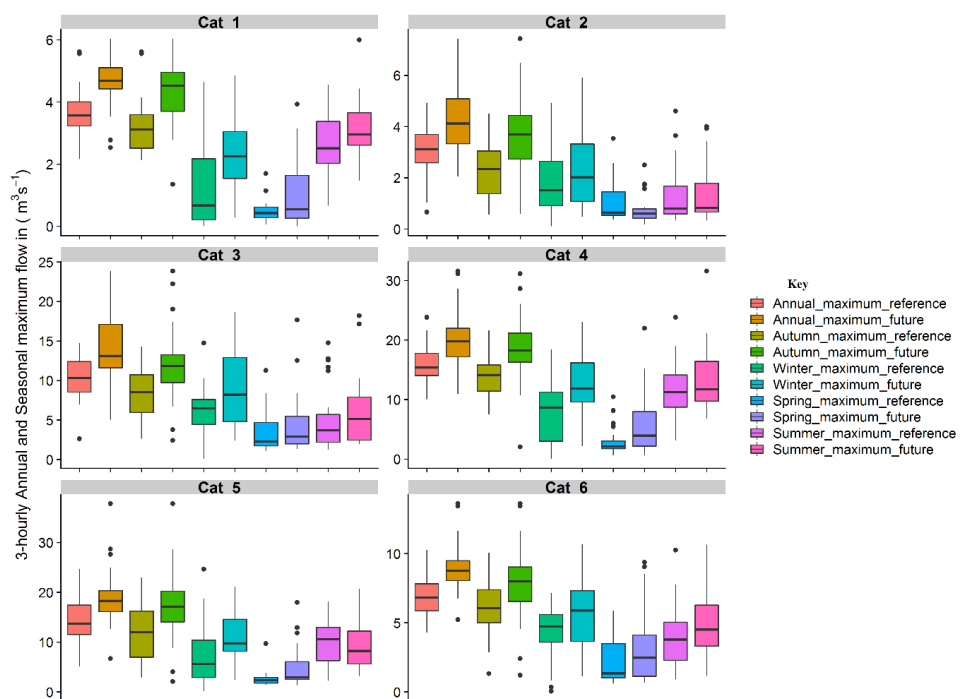


Figure 5. Distributions of the annual and seasonal maximum flow values of the 30 years period



Tables

Table 1: Catchment descriptors of the study catchments

Catchments Descriptors	Unit	Symbol	Catchments					
			Cat_1	Cat_2	Cat_3	Cat_4	Cat_5	Cat_6
Mean of distance distributions of soils in the catchment to the nearest river reach	<i>m</i>	D_m	103.0	169.1	204.3	137.0	174.9	171.7
Mean of distance distributions of marsh land in the catchment to the nearest river reach	<i>m</i>	D_{mr}	0.0	261.0	220.7	109.9	107.2	154.3
Mean of distance distribution of points in the river to the outlet	<i>m</i>	D_r	1513.2	960.5	2671.2	3061.1	3402.8	1733.3
Catchment area	km^2	A	1.5	2.3	7.3	7.9	8.2	3.8
Effective lake	%	L_e	0.2	0.0	0.0	0.7	0.0	0.0
Forest	%	F	18.5	65.3	75.8	22.5	69.7	25.4
Bare mountain	%	B	79.6	27.6	14.8	66.0	18.9	65.3
Urban	%	U	0.0	0.1	0.0	0.0	0.0	0.0
Mean elevation	<i>m</i>	M_e	684.6	322.1	314.7	461.5	402.1	466.7
Mean anual precipitation	<i>mm</i>	M_p	3268.0	2243.0	2500.0	2781.0	2543.0	2644.0
Speciifc discharge	$l s^{-1} km^{-2}$	S_q	141.0	115.7	91.8	125.6	134.2	110.7
Mean river slope	$m km^{-1}$	R_s	162.6	266.2	88.4	106.4	118.6	154.9
Outlet location								
ETRS_1989_UTM_Zone_33N coordinate system (m)	Longtiude		-9376.0	-14513.6	-15886.7	-22440.2	-14280.8	-25871.8
	Latitude		6777231.6	6712810.0	6758694.5	6725236.5	6719015.4	6732970.8



Table 2: Coefficients of the power relation between D_m and A_c and the coefficients of determination (R-squared).

Catchment_ID	a	b	R-squared
Cat_1	1.42	0.41	0.97
Cat_2	0.87	0.45	0.99
Cat_3	0.87	0.46	1
Cat_4	1.2	0.44	0.99
Cat_5	0.99	0.45	1
Cat_6	0.87	0.46	1



Table 3: DDD model parameters of the study catchments estimated from regionalization

Model parameters needing regionalization	Catchments					
	Cat_1	Cat_2	Cat_3	cat_4	Cat_5	cat_6
Gshape	2.317	1.827	1.977	2.087	1.961	2.032
Gscale	0.041	0.036	0.034	0.033	0.038	0.037
GshInt	4.085	3.083	3.39	3.615	3.356	3.502
GscInt	0.018	0.016	0.015	0.015	0.017	0.017
fc	49.3	122.1	140.00	68.30	134.2	69.00
Pro	0.1	0.087	0.082	0.100	0.095	0.096
Cx	0.155	0.129	0.108	0.137	0.159	0.147
CFR	0.004	0.006	0.007	0.004	0.003	0.004
Cea	0.033	0.025	0.016	0.032	0.028	0.031
rv	1.22	1.240	1.17	1.200	1.260	1.190



Table 4: Changes of mean annual temperature and precipitation, mean annual maximum snow water equivalent (SWE) and mean annual evapotranspiration for all the study catchments

Hydro-meteorological indicator	Unit	Change in indicator
<i>Cat_1</i>		
Mean annual precipitation	mm	22.2 %
Mean annual temprature	°c	3.3 °c
Mean annual maximum SWE	mm	-77.8 %
Mean annual evapotranspiration	mm	62.8 %
<i>Cat_2</i>		
Mean annual precipitation	mm	23.9 %
Mean annual temprature	°c	3.1 °c
Mean annual maximum SWE	mm	-47.5 %
Mean annual evapotranspiration	mm	66.5 %
<i>Cat_3</i>		
Mean annual precipitation	mm	23.64 %
Mean annual temprature	°c	3.2 °c
Mean annual maximum SWE	mm	-49.81 %
Mean annual evapotranspiration	mm	43 %
<i>Cat_4</i>		
Mean annual precipitation	mm	20.4 %
Mean annual temprature	°c	3.2 °c
Mean annual maximum SWE	mm	-56.05 %
Mean annual evapotranspiration	mm	131.5 %
<i>Cat_5</i>		
Mean annual precipitation	mm	22.1 %
Mean annual temprature	°c	3.2 °c
Mean annual maximum SWE	mm	-48.6 %
Mean annual evapotranspiration	mm	80.5 %
<i>Cat_6</i>		
Mean annual precipitation	mm	20.0 %
Mean annual temprature	°c	3.0 °c
Mean annual maximum SWE	mm	-63.0 %
Mean annual evapotranspiration	mm	91.8 %



Table 5: Changes in percentage of mean annual flow and seasonal flows of the study catchments. The unit of the flows is m³/s.

Hydrologic indicator (flow)	Change in indicator (%)	Hydrologic indicator (flow)	Change in indicator (%)
Cat_1		Cat_4	
Mean annual flow	33.3	Mean annual flow	16.5
Mean winter flow	256.3	Mean winter flow	167.7
Mean spring flow	48.9	Mean spring flow	99.7
Mean summer flow	3.6	Mean summer flow	-32.7
Mean Autumn flow	43.9	Mean Autumn flow	20.6
Cat_2		Cat_5	
Mean annual flow	21.9	Mean annual flow	18.9
Mean winter flow	41.3	Mean winter flow	146.7
Mean spring flow	-1.4	Mean spring flow	76.4
Mean summer flow	-7.2	Mean summer flow	-41.0
Mean Autumn flow	37.8	Mean Autumn flow	43.3
Cat_3		Cat_6	
Mean annual flow	21.9	Mean annual flow	17.0
Mean winter flow	68.3	Mean winter flow	81.1
Mean spring flow	4.3	Mean spring flow	10.0
Mean summer flow	-21.2	Mean summer flow	-35.2
Mean Autumn flow	41.1	Mean Autumn flow	35.1



Table 6: Winter/spring and fall center of volume dates for the six study attachments

Annual timing	Center volume (CV) date	Center volume (CV) date	Is CV date early or late?
<i>Cat_1</i>			
Winter/Spring	13 May	5 March	early
Fall	21 October	31 October	late
<i>Cat_2</i>			
Winter/Spring	18 March	2 March	early
Fall	11 November	12 November	late
<i>Cat_3</i>			
Winter/Spring	27 March	3 March	early
Fall	8 November	11 November	late
<i>Cat_4</i>			
Winter/Spring	24 April	10 march	early
Fall	29 October	8 November	late
<i>Cat_5</i>			
Winter/Spring	26 April	13 March	early
Fall	3 November	19 November	late
<i>Cat_6</i>			
Winter/Spring	11 April	3 March	early
Fall	8 November	11 November	late



Table 7: Changes in percentage of the mean annual and seasonal maximum flows in the future period compared to the reference period.

Annual and Seasonal maximum flows	Change in indicator (%)	Annual and Seasonal maximum flows	Change in indicator (%)
<i>Cat_1</i>		<i>Cat_4</i>	
Mean autumn maximum flow	37.7	Mean autumn maximum flow	33.1
Mean winter maximum flow	82.4	Mean winter maximum flow	59.8
Mean spring maximum flow	118.0	Mean spring maximum flow	105.5
Mean summer maximum flow	16.7	Mean summer maximum flow	17.7
Mean annual maximum flow	28.0	Mean annual maximum flow	28.9
<i>Cat_2</i>		<i>Cat_5</i>	
Mean autumn maximum flow	60.0	Mean autumn maximum flow	48.2
Mean winter maximum flow	32.2	Mean winter maximum flow	48.6
Mean spring maximum flow	-28.9	Mean spring maximum flow	86.4
Mean summer maximum flow	7.2	Mean summer maximum flow	1.1
Mean annual maximum flow	38.3	Mean annual maximum flow	31.4
<i>Cat_3</i>		<i>Cat_6</i>	
Mean autumn maximum flow	43.2	Mean autumn maximum flow	27.5
Mean winter maximum flow	45.7	Mean winter maximum flow	28.9
Mean spring maximum flow	25.4	Mean spring maximum flow	41.3
Mean summer maximum flow	20.7	Mean summer maximum flow	26.8
Mean annual maximum flow	36.9	Mean annual maximum flow	28.9



Table 8: Changes in the number of 3-hour floods which are greater than the minimum annual maximum flood in the reference period for all the study catchments.

Catchment ID	Mean annual number of 3-hours floods greater than the minimum annual maximum flood in the reference period		Changes in number (%)
	Reference period (1981-2011)	Future period (2070-2100)	
<i>Cat_1</i>	9.1	21.2	133.0
<i>Cat_2</i>	58	99.3	71.2
<i>Cat_3</i>	38	64.4	69.5
<i>Cat_4</i>	9	15.4	71.1
<i>Cat_5</i>	22.2	35.9	61.7
<i>Cat_6</i>	7	13.3	90



Table 9: Changes of flood frequencies with return periods of 2, 5, 10, 20, 25, 50, 100 and 200 years between the future and reference periods using Gumbel's Extreme Value Distribution for all study catchments.

T(years)	Change (%)					
	Cat_1	Cat_2	Cat_3	Cat_4	Cat_5	Cat_6
2	28.9	36.7	35.7	28.0	31.4	29.5
5	24.1	35.9	37.9	33.3	31.3	26.9
10	21.8	35.5	38.9	35.9	31.2	25.7
20	20.0	35.3	39.7	38.0	31.2	24.8
25	19.5	35.2	39.9	38.6	31.2	24.5
50	18.2	35.0	40.5	40.2	31.1	23.8
100	17.0	34.9	40.9	41.5	31.1	23.2
200	16.1	34.7	41.3	42.7	31.1	22.7